IEEE Access
Multidisciplinary | Rapid Review | Open Access Journal

Received June 27, 2018, accepted August 1, 2018, date of publication August 6, 2018, date of current version August 28, 2018.

Digital Object Identifier 10.1109/ACCESS.2018.2863745

Space-Range-Doppler Focus-Based Low-observable Moving Target Detection Using Frequency Diverse Array MIMO Radar

XIAOLONG CHEN, (Member, IEEE), BAOXIN CHEN, JIAN GUAN, (Member, IEEE), YONG HUANG, AND YOU HE

Radar Target Detection Research Group, Naval Aviation University, Yantai 264001, China

Corresponding author: Xiaolong Chen (cxlcxl1209@163.com)

This work was supported in part by the National Natural Science Foundation of China under Grant 61501487, Grant U1633122, Grant 61471382, and Grant 61531020, in part by the National Defense Science Foundation under Grant 2102024, in part by the Project of the Shandong Province Higher Educational Science and Technology Program under Grant J17KB139, in part by the National Key Research and Development Program under Grant 2016YFC0800406, and in part by the Young Elite Scientist Sponsorship Program of CAST and Special Funds of Taishan Scholars of Shandong.

ABSTRACT The radar echoes of moving targets in a clutter background are extremely weak and their characteristics are complex. A low-observable moving target detection technology has become a key constraint to radar performance, requiring the radar to provide flexible freedom and higher parameter estimation capabilities. In this paper, a frequency diverse array MIMO (FDA-MIMO) radar is used for moving target detection in a clutter background, which combines the information in spatial (azimuth)-range-frequency (Doppler) domains. Based on the signal model of the FDA-MIMO radar, a novel signal processing method is proposed named as space-range-Doppler focus (SRDF) processing. Theoretical and simulations analysis shows that this method can be regarded as the combination of multiple cascaded signal processing, such as beamforming, pulse compression, and Doppler filtering of a conventional array radar. It can distinguish clutter and moving targets in multidimensional space, improve signal-to-clutter ratio, and achieve high-precision measurement of target motion parameters via sparse time–frequency distributions. It will provide a new approach for moving target detection and classification in complex backgrounds.

INDEX TERMS Frequency diverse array MIMO (FDA-MIMO) radar, low-observable moving target, moving target detection, space-range-Doppler focus (SRDF), sparse time-frequency distribution (STFD).

I. INTRODUCTION

As the main means of target detection and surveillance, radar is widely used in public and defense security fields such as air and sea surface target monitoring and early warning detection [1]–[3]. However, due to the complex background environment, e.g., land, city, ocean, etc., and the complex motion characteristics of the target, radar echo is extremely weak, i.e., low observability [4], [5]. Low observable moving target detection technology in complex background has become the key constraint factor affecting the performance of radar and is also a worldwide difficulty. The key point is that in both time and frequency domain, the target's energy is very weak resulting in a low signal-to-noise/clutter ratio (SNR/SCR) [6]–[8]. On the one hand, from the point of view of clutter suppression, target detection in clutter firstly requires finding an observation space that can effectively separate the target and clutter. Based on this point, the observation space corresponding to signal processing gradually extends from the initial time domain to frequency domain [9], sparse domain [10], [11], time-frequency domain [12], and space-time domain [13], etc.. However, for a complex and dynamic background, it is necessary to further expand the dimensions of the observation space to provide more degrees of freedom (DoFs) for signal processing [14]. On the other hand, from the perspective of the target to be detected, radar detection is closely connected with complex and diverse types of targets [4], [15], which not only increases the complexity of radar signal processing, but also seriously affects the overall detection performance. The above problems require that the radar could provide more flexible DoFs, higher integration gain, better parameter estimation capabilities, and work robustly in various environments. One possible

and practical way is to accumulate target's energy in different domains [16]. However, commonly used radar, such as phased-array radar (PAR), often did this in space, range and Doppler domain separately. Therefore, it is necessary to investigate novel radar system and signal processing technology for moving target detection in complex environment.

The multiple-input multiple-output (MIMO) array radar has drawn great attentions recently for many advantages without sacrificing the excellence of the traditional PAR [17], [18]. Its flexibility in signal waveform and array element location can provide more DoFs for the signal processing in the complex and dynamic background. At the same time, its staring observation working mode can effectively reduce the dynamic range of the radar system, prolong the target observation time, improve the Doppler resolution, and thus help to accumulate the target energy with higher integration gain [19], [20]. However, MIMO radar also has its inherent drawback, e.g., in each scan snapshot, the beam pointing direction is fixed in the range, which means that the beam pointing is independent of the distance. In some applications, such as distance interference rejection or clutter suppression, it is often desired that array beams can point to different distances at a fixed angle within the same snapshot. That is to say the interferences or clutter located at the same angle but different ranges can be effectively suppressed by the range-dependent beamforming [21], [22], which is really hard for traditional PAR or MIMO radar.

In recent years, frequency diverse array (FDA) radar has gained substantial interests from researchers both at home and abroad [23], [24]. FDA radar transmits the same coherent signals as PAR, while the most obvious difference is that a small frequency increment, compared to the carrier frequency, is applied across the elements of FDA radar [25]. The frequency increment makes the beam direction change as a function of the range, angle, and time delay. After the center of the radiated signal is shifted a little, the antenna pattern of the array is distance-dependent. This would provide many advantages in interference rejection, resolution enhancement in synthetic aperture radar (SAR) imaging, and ambiguous range clutter suppression in space-time adaptive processing [26]–[29], etc..

Since the concept of FDA was firstly proposed by Antonik *et al. [30]*, at the international radar conference in 2006, the theory of FDA has been rapidly developed on array structure design, beamforming, range-angle joint parameter estimation, etc.. In 2007, Secmen analyzed the periodic modulation characteristics of FDA along the range and azimuth angles [31]. Sammartino *et al.* [32] used four frequency synthesizers to control four microstrip antennas and analyzed the beam patterns of FDA. In 2009, Higgins and Blunt [24] studied the application of continuous frequency modulation in the beam patterns of FDA and analyzed its ambiguity function. In 2010, Jones and Rigling [33] proposed a plane-structured FDA and a corresponding receiver implementation method. In 2015, Basit *et al.* [34] applied FDA to cognitive radar, and achieve the maximization of power by selecting the proper frequency offset. Khan *et al.* [35] used the log incremental frequency offset to obtain discontinuous beam patterns of FDA, and proposed using time-varying frequency offsets to solve the decoupling problem of range and angle. Chen *et al.* [29] studied the FDA beam pattern with pulse waveform, and pointed out the prerequisite for forming a stable point beam in space, which is helpful for real application of FDA radar. In 2017, IEEE Journal of Selected Topics in Signal Processing published a special issue ''Time/Frequency Modulation Array Signal Processing'', focusing on the progress of the array optimization, beamforming, parameter estimation, and SAR imaging for FDA radar [23], [36]–[38]. Theoretical researches show that FDA could provide new DoFs to control the transmitted energy distribution, making it a new and more advanced array antenna for future radar and navigation systems.

However, FDA cannot unambiguously estimate the target parameters due to the coupling problem of range and angle, which is a difficulty for signal integration and estimation. To overcome this problem, the advantages of FDA in range dependent transmit beampattern and MIMO in increased DoFs are jointly utilized, namely FDA-MIMO radar [39], [40]. At present, the researches on target detection of FDA or FDA-MIMO radar are mostly aimed at stationary targets or beamforming, localization for moving target [37], [41]. As for the signal processing of FDA-MIMO radar especially for moving target detection, further investigations are needed. Different from traditional target integration methods, where the target range, angle and Doppler are measured separately, FDA-MIMO radar has the potential ability of joint angle-range-Doppler estimation with samples during slow-time. For the moving target, especially for the maneuvering target with high-order motion, the time-varying characteristics of Doppler makes the energy divergence, i.e., Doppler migration, which makes it difficult for signal processing of FDA-MIMO radar.

In this paper, we propose a novel solution for moving target integration and detection using FDA-MIMO radar, which is named as space (angle)-range-Doppler focus (SRDF) processing. The advantages over the traditional methods and main contributions in the context of the proposed SRDF are summarized as follows:

1) In strong clutter background, the clutter amplitude is much higher than that of moving target, and their spectrums are overlapped with each other, i.e., it is rather difficult to separate them apart in both time and frequency domain. The proposed SRDF method makes full use of the flexible freedoms of space (azimuth), range, and frequency (Doppler) of FDA-MIMO radar to improve the detection capability of radar moving targets in complex environments. The FDA-MIMO spectrums of clutter and moving target are different in the SRDF domain, making it easy to distinguish them apart.

2) Traditional array radars, such as PAR and MIMO radar, whose beam pointing is independent of distance, make it difficult to achieve joint estimation of distance and azimuth. While using the proposed SRDF method, the energy of the

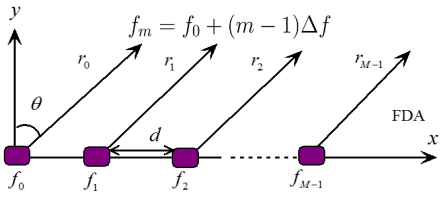

FIGURE 1. Transmit array of FDA radar.

moving target can be accumulated in the multi-dimensional space (range-angle-Doppler). Thus, the SNR/SCR can be improved with better anti-noise or anti-clutter ability.

3) For a non-uniformly moving target, it would come across the effect of Doppler migration using Fourier transform (FT)-based moving target detection (MTD) method, resulting in low integration gain and poor estimation accuracy. While in the finally step of the proposed SRDF-based detection method, we further develop the framework of sparse time-frequency distribution (STFD) [42], [43], and propose the sparse fractional Fourier transform (SFRFT) for high-resolution Doppler extraction of the non-uniformly moving target. Simulations verified the higher resolution than the traditional moving target detection (MTD) method.

The remaining of the paper is organized as follows. The signal model of FDA-MIMO radar is established in section II. In section III, we further investigate the three dimensional (3-D) SRDF model considering the Doppler information and then introduce the principle of SRDF processing. Also, the detailed detection procedure of FDA-MIMO radar is illustrated and compared with that of traditional PAR. Section IV shows the results of numerical simulations with noise and clutter and performances analysis for multiple moving targets, detection probability, and parameters estimation. The last section concludes the paper and presents its future research directions.

II. SIGNAL MODEL OF FDA-MIMO RADAR

The biggest difference between FDA radar and PAR is that there are small frequency increments in the carrier frequencies of adjacent FDA array elements. Considering a uniform linear array (ULA) with M transmit and N receiving elements, whose inter-element spacing is d, the structure of FDA is shown in Fig. 1.

Take the first transmit antennas as the reference point and the carrier frequency at the m th antenna is [30]

$$f_m = f_0 + \Delta f_m \tag{1}$$

where f_0 is the radar carrier frequency, The carrier frequency of each element increases linearly with a frequency increment $\Delta f_m = (m-1)\Delta f$.

The transmitted signal of the m th antenna can be written as

$$s_m(t) = w_m e^{j2\pi f_m t}, \quad m = 0, \cdots, M-1 \tag{2}$$

where w_m is the transmit weight. The synthesized signals arriving at a given far-field point target with angle-range pair

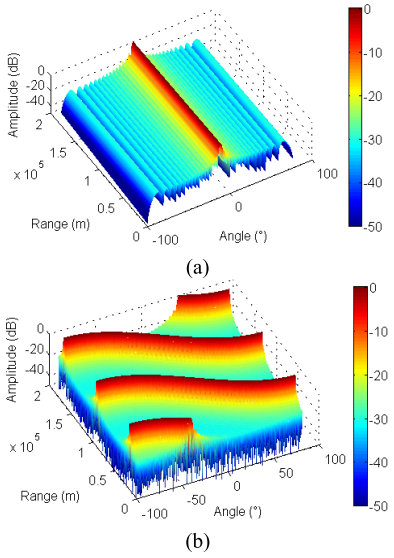

FIGURE 2. Transmit beampattern of FDA and PAR using continuous waveform. (a) PAR. (b) FDA.

(r, θ) can then be expressed as [23]

$$S(t; r, \theta) = \sum_{n=0}^{M-1} w_m^* s_m(t - \tau_m) \tag{3}$$

where $\tau_m = r_m/c_0$ denotes the signal propagation delay from the m th element to the target, with c_0 and $r_m = r - md\sin\theta$ being the speed of light and target slant range, respectively.

Following the narrow-band assumption, then (3) can be approximately expanded as

$$\begin{aligned} S(t; r, \theta) &= \sum_{n=0}^{M-1} w_m^* e^{-j2\pi(f_0+\Delta f_m)\left(t-\frac{r-md\sin\theta}{c_0}\right)} \\ &\approx e^{-j2\pi f_0(t-r/c_0)} \sum_{n=0}^{M-1} w_m^* e^{-j2\pi\Delta f_m(t-r/c_0)} \\ &\quad \times e^{-j2\pi f_0 md\sin\theta/c_0} \end{aligned} \tag{4}$$

The array factor at the position (r,θ) can be expressed as

$$\mathrm{AF}(t; r, \theta) = \sum_{n=0}^{M-1} w_m^* e^{-j2\pi\Delta f_m(t-r/c_0)} e^{-j2\pi f_0 md\sin\theta/c_0} \tag{5}$$

According to (5), Fig. 2 shows the transmit beampattern of FDA with $M = 32$, $\Delta f = 4$ kHz, and $f_0 = 9$ GHz, compared with a PAR. It is well recognized that FDA creates a range-angle-dependent beampattern whose amplitude and spatial distribution can be controlled by changing the frequency increments and the number of array elements.

The transmit beampattern of the pulsed FDA radar at different times is shown in Fig. 3, using $M = 10$, $f_0 = 5$ GHz, $d = 0.5\lambda$, $\Delta f = 1$ kHz, and the radar signal duration $T_p = 0.001$ s. The slight frequency increment of the FDA radar makes the transmitted beam related to the function of distance, azimuth and time. Making use of the

distance dependence of the antenna pattern, the transmitted beampattern can achieve local maximization along different distances. The beampattern of the pulsed FDA radar is a slanted line instead of an intermittent point, which indicates that the distance and angle of the FDA are coupled. This property is not conducive to the energy concentration of its mainlobe, and may easily cause signal leakage. The most practical decoupling approach is to jointly utilize FDA and MIMO, i.e., FDA-MIMO [39], [40]. In doing so, the range changing characteristics are produced by FDA and the angle changing characteristics are provided by MIMO. Then, both range and angle of the target can be unambiguously estimated via FDA-MIMO radar.

Suppose there is a target located as (r_s, θ_s), considering that the electromagnetic signals are independently propagating in free space, the far-field signal received by the n th element can then be represented by

$$y_{m,n}(r_s, \theta_s) = \alpha(r_s, \theta_s) e^{-j4\pi \Delta f_m r/c} e^{j2\pi md/\lambda \sin\theta} e^{j2\pi nd/\lambda \sin\theta} + c_{m,n} \quad (6)$$

where $\alpha(r_s, \theta_s)$ is the complex reflection coefficient, λ is the wavelength, $c_{m,n}$ is the clutter, $n = 0, \cdots, N-1$.

After pass-band filtering, the returned signal reflected by the far-field target can be concisely expressed by vector form,

$$\mathbf{y} = \alpha(r_s, \theta_s) [\mathbf{a}_{\mathrm{R}}(r_s) \odot \mathbf{a}_t(\theta_s)] \otimes \mathbf{a}_{\mathrm{r}}(\theta_s) + \mathbf{c} \quad (7)$$

where $\odot$ and $\otimes$ denote the Hadamard (element-wise) product and Kronecker product operators respectively. $\mathbf{a}_{\mathrm{t}}(\theta_s)$, $\mathbf{a}_{\mathrm{r}}(\theta_s)$, and $\mathbf{a}_{\mathrm{R}}(r_s)$ are the transmit, receive, and transmit range steering vectors, respectively. They have the forms of [37]

$$\mathbf{a}_{\mathrm{t}}(\theta_s) = \left[1 \quad e^{\mathrm{j}2\pi df_0/c_0 \sin\theta_s} \quad \cdots \quad e^{\mathrm{j}2\pi(M-1)df_0/c_c \sin\theta_s} \right]^T \quad (8)$$

$$\mathbf{a}_{\mathrm{r}}(\theta_s) = \left[1 \quad e^{\mathrm{j}2\pi df_0/c_0 \sin\theta_s} \quad \cdots \quad e^{\mathrm{j}2\pi(N-1)df_0/c_0 \sin\theta_s} \right]^T \quad (9)$$

$$\mathbf{a}_{\mathrm{R}}(r_s) = \left[e^{-\mathrm{j}4\pi \Delta f_0 r_s/c_0} \quad e^{-\mathrm{j}4\pi \Delta f_1 r_s/c_0} \quad \cdots \quad e^{-\mathrm{j}4\pi \Delta f_{M-1} r_s/c_0} \right]^T \quad (10)$$

where, ^{T} is conjugate transpose operator. As shown in (7), the transmit steering vector is not only angle-dependent but also range-dependent. Let

$$\mathbf{a}(r_s, \theta_s) = [\mathbf{a}_{\mathrm{R}}(r_s) \odot \mathbf{a}_t(\theta_s)] \otimes \mathbf{a}_{\mathrm{r}}(\theta_s) \quad (11)$$

Then for the received signal of a FDA-MIMO radar, the range, transmit, and receive steering vectors have the following form after mixed, sampled, and filtering.

$$\mathbf{y}\, \alpha(r_s, \theta_s) \mathbf{a}(r_s, \theta_s) + \mathbf{c} \quad (12)$$

As can be seen from the above equation, the coupling between range and angle is perfectly solved, indicating that FDA-MIMO radar has a naturally decoupling capability. Therefore, it could utilize the transmit and receive DoFs to determine the range and angle of the target.

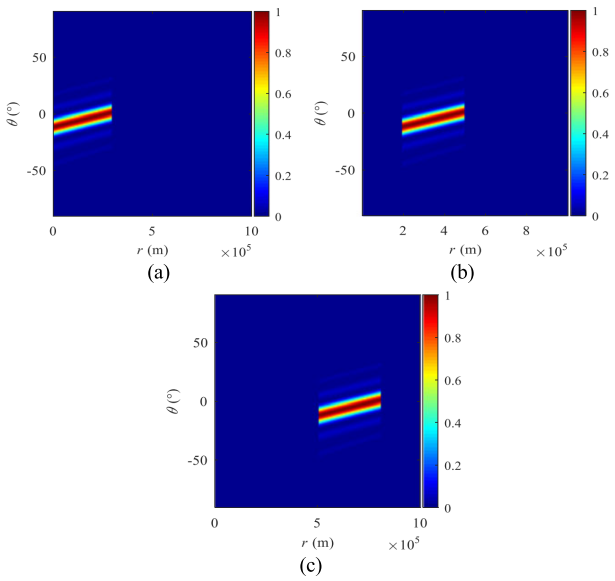

FIGURE 3. Transmit beampattern of pulsed FDA radar at different times [29]. (a) $t = 0.001$s. (b) $t = 0.0017$s. (c) $t = 0.0027$s.

III. PRINCIPLE OF SRDF AND MOVING TARGET DETECTION

A. 3-D SRDF MODEL OF FDA-MIMO RADAR

Now, we further establish the 3-D SRDF signal model, i.e., in case of a moving target, which is an extension of the previous model (12). Suppose the hypothetical target has a radial velocity vr, which results in a Doppler frequency shift fd in the returned signals. The FDA-MIMO radar transmits continuous waveform to detect the moving target. The frequency increment Δf adopted in the FDA-MIMO radar is relatively negligible while compared with f_0 and the waveform bandwidth, and thus, the Doppler frequency shift due to Δf can be ignored. Following (7), the signal model for the moving target can be revised as

$$\mathbf{y}_{\mathrm{mov}} = \alpha(r_s, \theta_s, f_{\mathrm{d}}) [\mathbf{a}_{\mathrm{d}}(f_{\mathrm{d}}) \otimes \mathbf{a}(r_s, \theta_s)] + \mathbf{c} \quad (13)$$

where $\alpha(r_s, \theta_s, f_{\mathrm{d}})$ is the complex reflection coefficient, $\mathbf{a}_{\mathrm{d}}(f_{\mathrm{d}})$ is the Doppler vector in the slow time, given by

$$\mathbf{a}_{\mathrm{d}}(f_{\mathrm{d}}) = \left[1 \quad e^{j2\pi f_{\mathrm{d}} T_p} \quad \cdots \quad e^{\mathrm{j}2\pi(L-1) f_{\mathrm{d}} T_p} \right]^T \quad (14)$$

Where L is the sampling number. Let

$$\boldsymbol{\kappa}_{\mathrm{mov}}(r_s, \theta_s, f_{\mathrm{d}}) = \mathbf{a}_{\mathrm{d}}(f_{\mathrm{d}}) \otimes \mathbf{a}(r_s, \theta_s) \quad (15)$$

then

$$\mathbf{y}_{\mathrm{mov}} = \alpha(r_s, \theta_s, f_{\mathrm{d}}) \boldsymbol{\kappa}_{\mathrm{mov}}(r_s, \theta_s, f_{\mathrm{d}}) + \mathbf{c} \quad (16)$$

where $\boldsymbol{\kappa}_{\mathrm{mov}}(r_s, \theta_s, f_{\mathrm{d}})$ can be viewed as a joint angle-range-Doppler steering vector in the slow time. If the target moves with constant velocity, then, $f_{\mathrm{d}} = 2v_0/\lambda$, and $f_{\mathrm{d}} = 2(v_0 + a_s t_m)/\lambda$ for the accelerated moving target, where t_m denotes the slow time related to the Doppler processing.

It can be seen from the above equation that the joint estimation of angle-range-Doppler can be realized by using

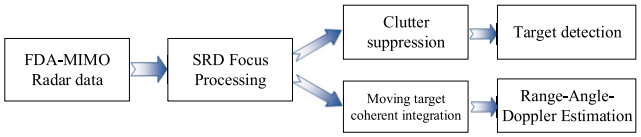

FIGURE 4. FDA-MIMO radar signal processing via SRDF processing.

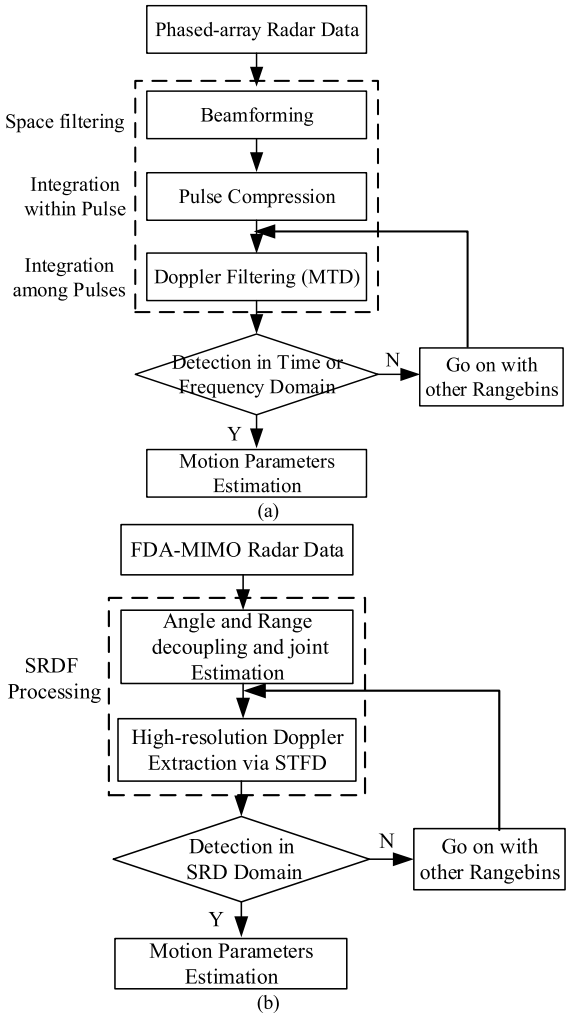

FIGURE 5. Flowchart of moving target detection. (a) PAR. (b) FDA-MIMO Radar.

FDA-MIMO radar for moving targets. The range and Doppler of the moving target can be jointly estimated and accumulated with the L samples. Combined with the long-time degree of MIMO, the Doppler resolution of the echo signal can be greatly improved. Therefore, FDA-MIMO radar has SRD 3-D focus processing capabilities, which helps further improve the SNR/SCR and obtain the refined characteristics of the low-observable moving target.

B. SRDF PROCESSING ARCHITECTURE

From (16), it can be seen that the essence of $\kappa_{\mathrm{mov}}(r_s, \theta_s, f_{\mathrm{d}})$ is angle, range, and Doppler focusing factors both in fast and slow time. Therefore, for moving targets, making use of the distance-azimuth joint estimation characteristic and the long-time DoFs in slow-time of the FDA-MIMO radar, the joint processing of space (azimuth)-distance (range for fast time)-frequency (Doppler for slow time) can be realized. Correspondingly, SNR/SCR could be further improved due to integration among multi-dimensions, which is helpful for the detection of low observable moving targets. The signal processing flowcharts of FDA-MIMO radar and traditional PAR are shown in Fig. 4 and Fig. 5. The main advantages of SRDF of FDA-MIMO radar are summarized as follows:

1) The traditional cascaded signal processing procedures, e.g., beamforming (angle estimation), pulse compression (range measurement), and Doppler banks filtering (Coherent integration), etc., can be replaced by SRDF processing of FDA-MIMO radar, which is realized by (16).

2) Energy of the moving target is accumulated in the three-dimensional (3-D) domains after SRDF processing. Moreover, moving target, clutter, and jamming can be separated in the 3-D dimensions, which would be a promising solution for clutter suppression and jamming rejection. This part is verified in section IV(b).

3) The SRDF processing completes the estimation of the space (range and angle) and motion parameters with high-precision, which would be verified in section IV(c). Acquisition of target spatial parameters and motion parameters via SRDF can provide important and refined features of the target, which may lay a good foundation for the subsequent identifications.

In short, the propose SRDF signal processing method of FDA-MIMO radar in this paper would provide a promising solution for improving the radar moving target detection performance in complex environment.

C. SRDF-BASED MOVING TARGET DETECTION METHOD

Figure 5(b) gives the flowchart of SRDF-based low-observable moving target detection and estimation with FDA-MIMO radar. It mainly consists of five procedures.

Step 1: Get the FDA-MIMO radar data from multiple receiving elements and perform the pass-band filtering [38]. Then we got the range-angle vector of receiving array signal, i.e., (12).

Step 2: Range and angle decoupling.

The decoupling problem of range and angle can be well solved by FDA-MIMO radar and joint estimation can be achieved by the spatial spectrum estimation. Some subspace algorithms such as MUSIC, estimation of signal parameters via rotation invariance (ESPRIT), Capon can be applied for range-angle estimation [44], [45].

Considering the additive clutter $\mathbf{c}$, independent and identically distributed, with a zero mean variance σ_c^2 Gaussian distribution, the covariance matrix of the received signal vector $\mathbf{y}$ of the FDA-MIMO radar is represented as

$$\mathbf{R}_{\mathbf{y}} = E\left[\mathbf{y}\mathbf{y}^H\right] = \sum_i \alpha_i^2(r_i, \theta_i)\mathbf{a}(r_i, \theta_i)\mathbf{a}^H(r_i, \theta_i) + \sigma_c^2\mathbf{I} \quad (17)$$

where ^{H} is a conjugate transpose operation. Suppose the target and clutter are independent, then the covariance matrix is rewritten as

$$\mathbf{R}_{\mathbf{y}} = (\mathbf{U}_{\mathrm{T}}|\mathbf{U}_c)\begin{pmatrix} \Lambda + \sigma_c^2\mathbf{I} & 0 \\ 0 & \sigma_c^2\mathbf{I} \end{pmatrix}(\mathbf{U}_{\mathrm{T}}|\mathbf{U}_c)^H \tag{18}$$

where, Λ is the diagonal matrix composed of the eigenvalues of the target signal matrix. The corresponding eigenvectors of $\Lambda + \sigma_c^2\mathbf{I}$ constitute the signal subspace $\mathbf{U}_{\mathrm{T}}$, and the corresponding eigenvectors of $\sigma_c^2\mathbf{I}$ constitute the clutter subspace. Since the clutter is orthogonal to the signal subspace, the spectrum function for the FDA-MIMO radar is as follows.

$$P_{\text{FDA-MIMO}} = \frac{1}{\mathbf{a}^H(r,\theta)\mathbf{U}_{\mathrm{n}}\mathbf{U}_{\mathrm{n}}^H\mathbf{a}(r,\theta)} \tag{19}$$

Then, the distance and angle of the moving target can be determined by searching the peak of the spectrum.

Step 3: High-resolution Doppler extraction via STFD.

Due to the complex motion of moving target, the Doppler may exhibit time-varying properties, and during long observation time, the computational cost of SRDF processing may increase exponentially for multiple transmitting, receiving channels and Doppler samples. Then how to obtain high integration gain and Doppler resolution of moving target and at the same time reduce the computational burden is the key point for SRDF processing of FDA-MIMO radar. In this paper, we adopt the idea of STFD method and propose the SFRFT-based method for high resolution Doppler extraction. Making use of the sparse characteristic of the moving target, the local optimization idea of sparse decomposition is introduced to the time-frequency analysis, i.e., STFD, which can effectively improve the operation efficiency, time-frequency resolution and parameter estimation performance for low-observable moving target modelled as time-varying signal.

For the sparse representation of the signal, the set $\mathbf{g} = \{g_j; j = 1, 2, \ldots, J\}$, whose elements are the unit vectors of the entire Hilbert space $H = R^P$ $(J \geq P)$, is called as the dictionary. The elements in the dictionary are atoms. For any signal $\mathbf{y} \in H$, it can be expanded into a linear combination of a set of atoms, i.e.,

$$\mathbf{y} = \sum_{j=1} \beta_j g_j \tag{20}$$

where j is the number of atoms, and the coefficient β_j denotes the similarity of the signal and the atoms.

The over-complete chirp basis is used to form dictionary for sparse representation. i.e.,

$$\mathbf{G}_s = \begin{bmatrix} g_s(f_1,\mu_1) & g_s(f_1,\mu_2) & \cdots & g_s(f_1,\mu_{L_2}) \\ g_s(f_2,\mu_1) & g_s(f_2,\mu_2) & \cdots & g_s(f_2,\mu_{L_2}) \\ \vdots & \vdots & \vdots & \vdots \\ g_s(f_{L_1},\mu_1) & g_s(f_{L_1},\mu_2) & \cdots & g_s(f_{L_1},\mu_{L_2}) \end{bmatrix} \tag{21}$$

$$\begin{aligned} &g_s(f_l,\ \mu_k) \\ &\quad = \exp\left(\mathrm{j}2\pi f_l t_m + j\pi\mu_k t_m^2\right), \\ &\qquad l = 1, 2, \ldots, L_1;\ k = 1, 2, \ldots, L_2 \end{aligned} \tag{22}$$

where $f_l = 2v_l/\lambda$, v_l is the initial velocity, and $\mu_k = 2a_k/\lambda$, a_k is the acceleration of the moving target.

The expected searching scope of the center frequency is $f_l \in [f_1, f_2]$, according to varieties of targets to be detected, and the interval depends on the Doppler resolution, that is, $\Delta f = 2/T_n$. Therefore, the number of searching velocity is $L_1 = \lceil (f_2 - f_2)T_n/2 \rceil$, where $\lceil\rceil$ denotes the round up to an integer operation. $[\mu_1, \mu_2]$, interval $\Delta\mu$, and searching number L_2 are determined in the same way, i.e., $\Delta\mu = 2/T_n^2$, $L_2 = \left\lceil (\mu_2 - \mu_2)T_n^2/2 \right\rceil$. Therefore, the chirp dictionary is a $L_1 \times L_2$ matrix.

Rewrite the signal model as the function of slow-time and frequency (t_m, f), and the signal along the range-angle unit (r_i, θ_i) of FDA-MIMO radar returns after the step 2 can be expressed as $y_{\mathrm{mov}}(t_m)|_{(r_i,\theta_i)}$, whose STFD $\rho_{\mathbf{y}}(t_m, f)|_{(r_i,\theta_i)}$ has the following form

$$\rho_{\mathbf{y}}(t_m, f)|_{(r_i,\theta_i)} = \sum_{k=1} a_k^2(t_m)\delta\left[f - \dot{\varphi}_k(t_m)/2\pi\right] \tag{23}$$

where $\dot{\varphi}_k(t_m)$ is the estimation of the signal frequency. For example, $\dot{\varphi}(t_m) = f_0 + \mu_s t_m$ for the accelerated moving target.

Rewrite the above expression by the form of sparse representation, and then we got the following expression

$$\rho_{\mathbf{y}}(t_m, f)|_{(r_i,\theta_i)} = \sum_{j=1} \beta_j(t_m) g_j(t_m, f) \tag{24}$$

where $g_j(t_m, f)$ is the atoms.

The sparse representation of (24) can be regarded as the optimization problem and solved by l_1-norm minimization, i.e.,

$$\begin{aligned} \rho_{\mathbf{y}}|_{(r_i,\theta_i)} = &\arg\min_{\rho_{\mathbf{y}}} \left\|\rho_{\mathbf{y}}(t_m, f)|_{(r_i,\theta_i)}\right\|_1, \\ &\text{s.t. } o\left\{\rho_{\mathbf{y}}(t_m, f)|_{(r_i,\theta_i)}\right\} = b \end{aligned} \tag{25}$$

where b is the constant, and o stands for the sparse operator with $J \times P$ dimension. The above equation can be relaxed by the following constraint, i.e.,

$$\begin{aligned} \rho_{\mathbf{y}}|_{(r_i,\theta_i)} = &\arg\min_{\rho_{\mathbf{y}}} \left\|\rho_{\mathbf{y}}(t_m, f)|_{(r_i,\theta_i)}\right\|_1, \\ &\text{s.t. } \left\|o\left\{\rho_{\mathbf{y}}(t_m, f)|_{(r_i,\theta_i)}\right\} - b\right\|_2 \leq \varepsilon \end{aligned} \tag{26}$$

When $\varepsilon = 0$, (25) and (26) have the same form. And when o and b stand for the FRFT and the amplitude of FRFT respectively, the SFRFT can be represented as

$$\begin{aligned} \mathcal{F}^{\alpha}|_{(r_i,\theta_i)} = &\arg\min_{\mathcal{F}^{\alpha}} \left\|\mathcal{F}^{\alpha}(t_m, f)|_{(r_i,\theta_i)}\right\|_1, \\ &\text{s.t. } \left\|o\left\{\mathcal{F}^{\alpha}(t_m, f)|_{(r_i,\theta_i)}\right\} - f(\alpha, u)\right\|_2 \leq \varepsilon \end{aligned} \tag{27}$$

where $\mathcal{F}^{\alpha}(t_m, f)$ is the SFRFT spectrum, $\alpha \in (0, \pi]$ denotes transform angle and u means the SFRFT domain. The relation

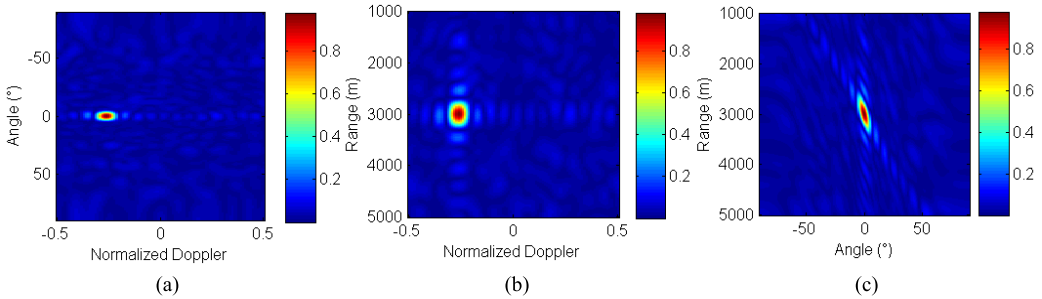

FIGURE 6. Spatial spectrum of uniformly moving targets in a noise background for FDA-MIMO radar (SNR = 0 dB). (a) Doppler versus azimuth. (b) Doppler versus range. (c) Range versus azimuth.

between (α, u) and the central frequency, chirp rate (f, μ) is

$$\begin{cases} f = u \csc \alpha \\ \mu = -\cot \alpha \end{cases} \tag{28}$$

The over-complete dictionary described by (21) is taken as the sparse representative dictionary of SFRFT. It should be noted that the proposed SFRFT can be generally calculated by the sparse optimization algorithms such as the basis pursuit denoising (BPDN) [46]. And it also can be achieved by the sparse fast FT (SFFT)-based method for higher efficiency in case of huge computations [47], [48], e.g., more than 2^{12} samples.

Step 4: Go through all the detection units and achieve moving target detection in SRD domain.

If all the searching parameters are traversed, we will obtain the detection map in the SRD domain, i.e., $\left|\mathcal{F}^{\alpha}(t_m, f)|_{(r_i,\theta_i)}\right|$, which means the peak value in the SRD domain for different searching unit (r_i, θ_i). We take the modulus as test statistic and compare with an adaptive threshold.

$$\{\alpha_0, u_0\} = \arg\max_{\alpha,u} \left|\mathcal{F}^{\alpha}(t_m, f)|_{(r_i,\theta_i)}\right| \underset{H_1}{\overset{H_0}{\gtrless}} \eta \tag{29}$$

where η is the threshold usually determined by a commonly used detector. If the test statistic is bigger than the threshold, a moving target in the (r_i, θ_i) bin can be declared. Otherwise, go on with the other detection bins. The peak coordinate (α_0, u_0) corresponds to the central frequency and chirp rate of the signal from a moving target, i.e.,

$$(f_0, \mu_s) = (u_0 \csc \alpha_0, -\cot \alpha_0) \tag{30}$$

Step 5: Target's motion parameters estimation.

Finally, estimate the motion parameters, such as initial velocity $\hat{v}_0$, acceleration $\hat{a}_s$, according to the detected peak location in the SRD domain.

$$\begin{cases} \hat{v}_0 = \dfrac{\lambda}{2} u_0 \csc \alpha_0 \\ \hat{a}_s = -\dfrac{\lambda}{2} \cot \alpha_0 \end{cases} \tag{31}$$

Then the high-resolution estimation of range, angle, and velocity of moving target is completed and the SRDF is achieved.

IV. SIMULATION AND RESULTS ANALYSIS

In order to validate the superior performances of the proposed SRDF method on low-observable moving target detection and estimation, this section gives numerical experiments. We set two kinds of targets, i.e., uniformly and accelerated moving target, in different environments, noise and clutter. Also, the SRDF detection method of FDA-MIMO radar is compared with the method via PAR.

A. SRDF IN NOISE BACKGROUND

In the simulations, we consider that the FDA-MIMO radar transmits continuous signal, including $M = 16$ transmit elements and $N = 16$ receive elements. For each channel, $L = 16$ samples are collected during the coherent processing interval with sampling frequency $f_s = 1000$ Hz. The reference carrier frequency is $f_0 = 1$ GHz while the frequency increment of FDA-MIMO is $\Delta f = 30$ kHz. The SNR = 0 dB and -15 dB, and the target is assumed at the slant range 3km with two uniformly velocity, i.e., $v_0 = -39$m/s (-260 Hz), and accelerated velocity, i.e., $v_0 = -39$m/s (-260 Hz), $a_s = 2\text{m/s}^2$ (13.4 Hz/s), respectively.

Fig. 6-Fig. 9 show spatial spectrum of FDA-MIMO radar for moving target with uniformly and accelerated velocity, including angle-Doppler spectrum, range-Doppler spectrum, and range-angle spectrum, respectively. The axis of Doppler is normalized. Compared with the FDA-MIMO spectrum for the two kinds of moving target, the following points can be concluded:

1) Different from the stationary target, the FDA-MIMO spectrum of the moving target has a Doppler shift corresponding to the motion status.

2) The Doppler spectrum of the non-uniformly moving target diverges across multiple Doppler units, i.e., Doppler migration, which is not conducive to the accumulation of target energy and the estimation of the motion parameters.

3) With the decrease of SNR, the noise amplitude is enhanced, but it is easy to detect the moving target via the angle-Doppler or range-Doppler spectrum. Moreover, we can find the output of the spectrum related with Doppler information is better than the range versus azimuth spectrum. This is because that the energy of moving target is accumulated

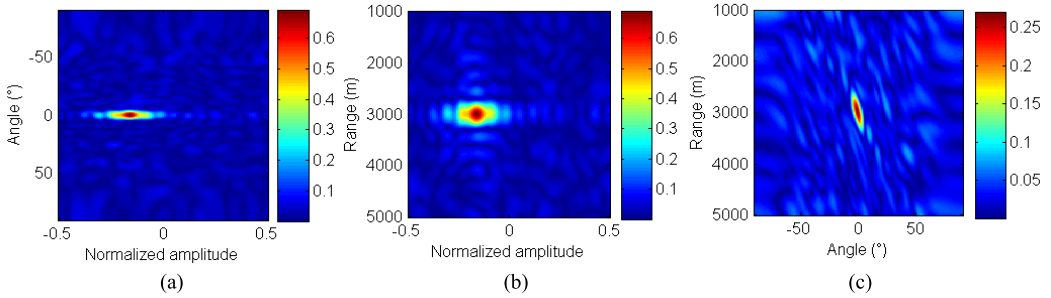

FIGURE 7. Spatial spectrum of accelerated moving targets in a noise background for FDA-MIMO radar (SNR = 0 dB). (a) Doppler versus azimuth. (b) Doppler versus range. (c) Range versus azimuth.

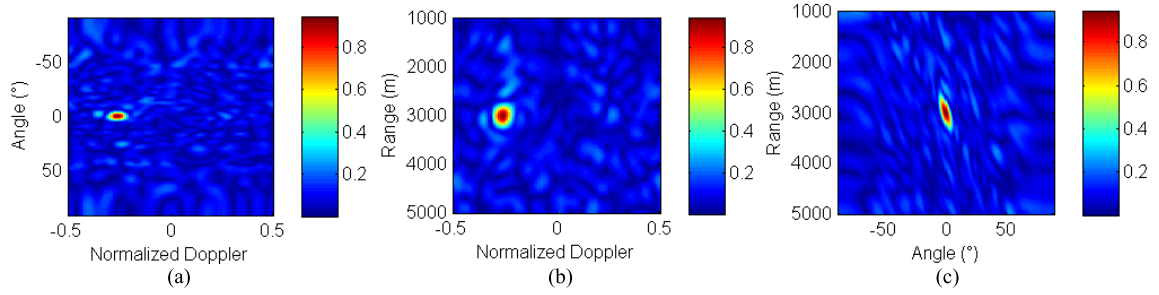

FIGURE 8. Spatial spectrum of uniformly moving targets in a noise background for FDA-MIMO radar (SNR = −15 dB). (a) Doppler versus azimuth. (b) Doppler versus range. (c) Range versus azimuth.

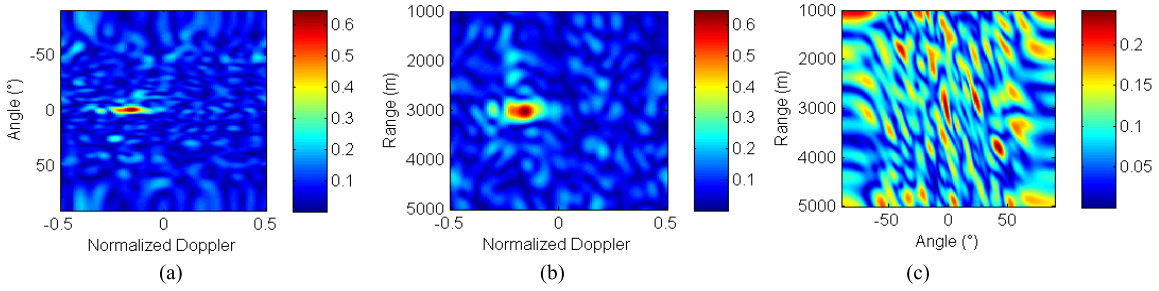

FIGURE 9. Spatial spectrum of accelerated moving targets in a noise background for FDA-MIMO radar (SNR = −15 dB). (a) Doppler versus azimuth. (b) Doppler versus range. (c) Range versus azimuth.

in the Doppler domain with improved SNR, which is better for low-observable moving target detection. From the above analysis, the three-dimensional joint processing for range, angle, and Doppler can be realized by the FDA-MIMO radar.

In order to overcome the effects of Doppler migration for non-uniformly moving target for better Doppler resolution, we perform the SRDF processing according to the flowchart of Fig. 5(b), and STFD are employed for high-resolution sparse representation. Fig. 10-Fig. 13 are the FDA-MIMO spectrum at the target's rangabin for different SNRs. The SFT and SFRFT are used for Doppler focusing and high resolution sparse processing for different motion states. The peak value of the target is obvious, thus overcoming the Doppler migration effect of the FDA-MIMO spectrum for maneuvering target. Therefore, 3D integration of moving target can be achieved with high-resolution using SRDF processing.

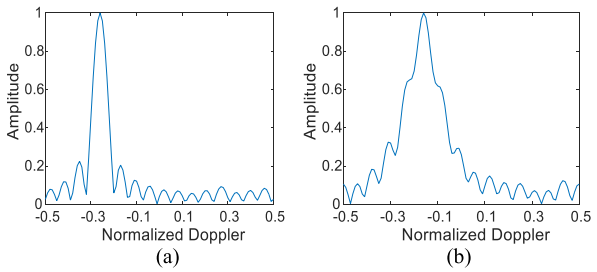

FIGURE 10. FDA-MIMO spectrum at the target's rangabin (SNR = 0 dB). (a) Uniformly moving target. (b) Accelerated moving target.

B. SRDF IN CLUTTER BACKGROUND

In this part, the performances in clutter background of the proposed SRDF processing for FDA-MIMO radar are verified. Clutter data obeying Weibull distribution is added to the

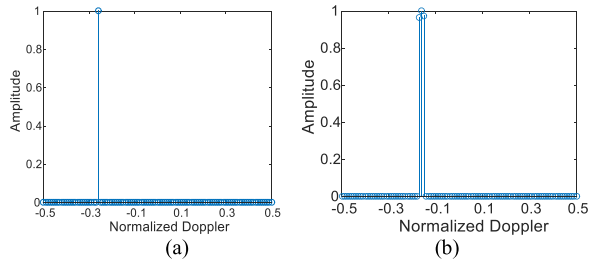

FIGURE 11. FDA-MIMO spectrum at the target's rangabin via STFD (SNR = 0 dB). (a) Uniformly moving target (SFT). (b) Accelerated moving target (SFRFT).

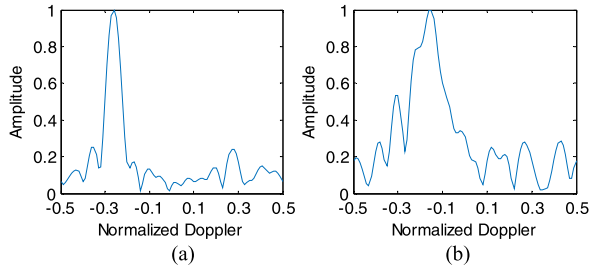

FIGURE 12. FDA-MIMO spectrum at the target's rangabin (SNR = −15 dB). (a) Uniformly moving target. (b) Accelerated moving target.

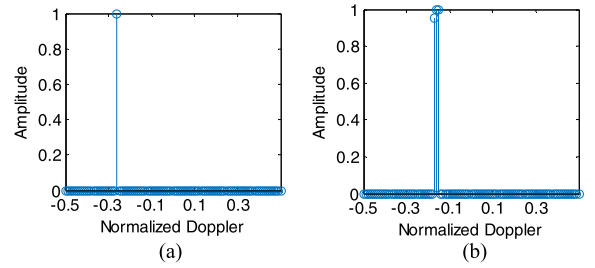

FIGURE 13. FDA-MIMO spectrum at the target's rangabin via STFD (SNR = −15 dB). (a) Uniformly moving target (SFT). (b) Accelerated moving target (SFRFT).

simulated moving target and also simulations for two SCRs, i.e., 0 dB and −15 dB. Compared with the FDA-MIMO spectrum in noise background, it can be found that the power of clutter background is higher than that of the noise and we give the spatial spectrum of moving target in clutter background in dB, which is shown in Fig. 14-Fig. 17. Traditionally, the spectrum of clutter should be mixed with target together, e.g. using PAR, while for FDA-MIMO radar, they can be separated in Doppler and range domain (see Fig. 14(b)-Fig. 17(b)). This is because that clutter is distributed around zero range 'frequency' (refer to (13)) and zero Doppler frequency. That is to say that using FDA-MIMO radar, clutter would appear at the same angle but different ranges with the target, and can be effectively suppressed, while it won't work for traditional PAR or MIMO radar. Therefore, this advantage can be used for moving target detection in strong clutter background, e.g., sea environment. Then, FDA-MIMO spectrum at the target's rangabin with SCR = −15 dB is shown in Fig. 18 and Fig. 19. Because the clutter and moving target can be separated along the range and Doppler direction, the Doppler spectrum

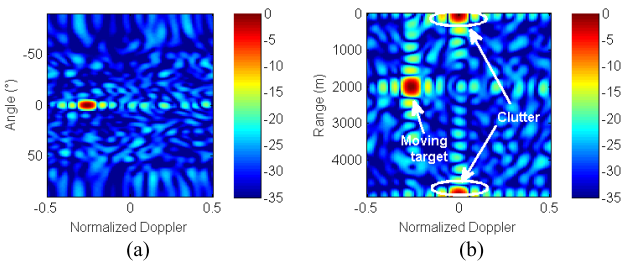

FIGURE 14. Spatial spectrum of uniformly moving targets in clutter background for FDA-MIMO radar (SCR = 0 dB). (a) Doppler versus azimuth (dB). (b) Doppler versus range (dB).

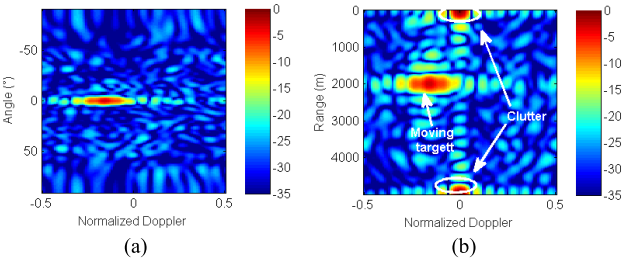

FIGURE 15. Spatial spectrum of accelerated moving targets in clutter background for FDA-MIMO radar (SCR = 0 dB). (a) Doppler versus azimuth (dB). (b) Doppler versus range (dB).

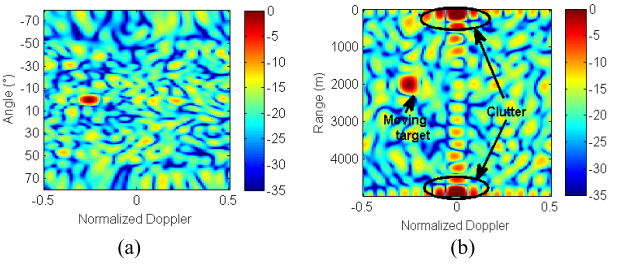

FIGURE 16. Spatial spectrum of uniformly moving targets in clutter background for FDA-MIMO radar (SCR = −15 dB). (a) Doppler versus azimuth (dB). (b) Doppler versus range (dB).

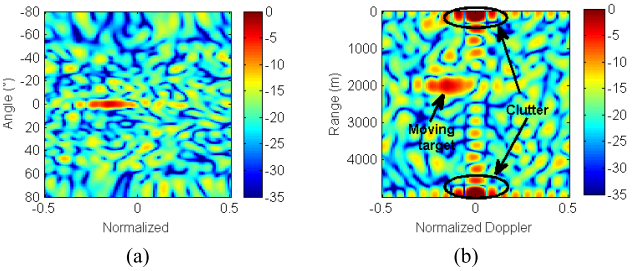

FIGURE 17. Spatial spectrum of accelerated moving targets in clutter background for FDA-MIMO radar (SCR = −15 dB). (a) Doppler versus azimuth (dB). (b) Doppler versus range (dB).

amplitude of clutter is still lower than the moving target resulting in good performance for SRDF.

C. PERFORMANCES ANALYSIS

1) FDA-MIMO SPECTRUM OF MULTIPLE MOVING TARGETS

FDA-MIMO spatial spectrum of multiple targets is shown in Fig. 20, and we set two scenarios: one is the same azimuth, different range and Doppler, i.e., $\theta_1 = \theta_2 = 0°$, $r_1 = 2990$m,

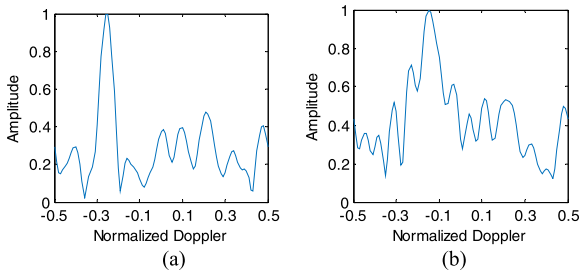

FIGURE 18. FDA-MIMO spectrum at the target's rangabin (SCR = −15 dB). (a) Uniformly moving target. (b) Accelerated moving target.

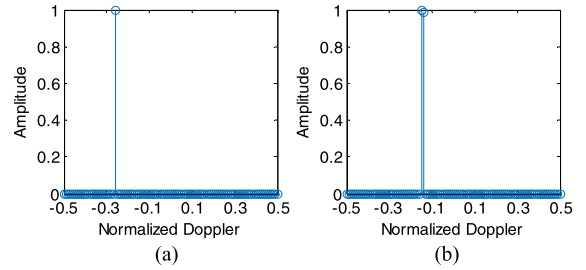

FIGURE 19. FDA-MIMO spectrum at the target's rangabin via STFD (SCR = −15 dB). (a) Uniformly moving target (SFT). (b) Accelerated moving target (SFRFT).

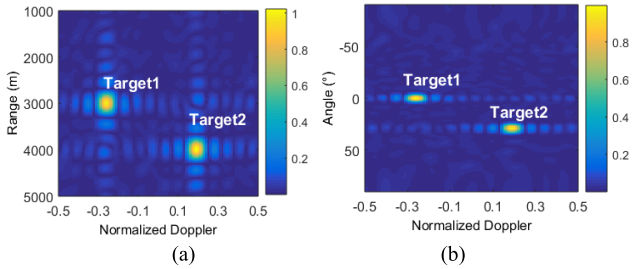

FIGURE 20. FDA-MIMO spatial spectrum of multiple targets (SNR = 0 dB). (a) The same azimuth, different range and Doppler. ($\theta_1 = \theta_2 = 0°, r_1 = 2990$m, $r_2 = 3990$m, $f_{d1} = -0.26$, $f_{d2} = 0.19$). (b) The same range, different azimuth and Doppler. ($r_1 = r_2 = 2990$m, $\theta_1 = 0°$, $\theta_2 = 29°$, $f_{d1} = -0.26$, $f_{d2} = 0.19$).

$r_2 = 3990$m, $f_{d1} = -0.26$, $f_{d2} = 0.19$, the other is the same range, different azimuth and Doppler, i.e., $r_1 = r_2 = 2990$m, $\theta_1 = 0°$, $\theta_2 = 29°$, $f_{d1} = -0.26$, $f_{d2} = 0.19$. It can be found that utilizing the spatial spectrum of FDA-MIMO radar, multiple targets can be distinguished in angle, distance, and Doppler multi-dimensions.

2) DETECTION PERFORMANCES UNDER DIFFERENT SCRs

The simulated detection probabilities P_d of the PAR and FDA-MIMO are computed with 10^5 runs at each SNR to obtain the corresponding $P_{fa} = 10^{-3}$. The signal procedures of the two radars are carried out according to the flowcharts in Fig. 5. Uniformly and accelerated moving targets embedded in Weibull clutter background are considered. The SCR is incremented in 1 dB interval between −25 dB and 5 dB. The biparameter detector is employed in the SRDF domain. The curves of P_d versus SCR of PAR and FDA-MIMO radar are shown in Fig. 21. Since more DoFs (samples from

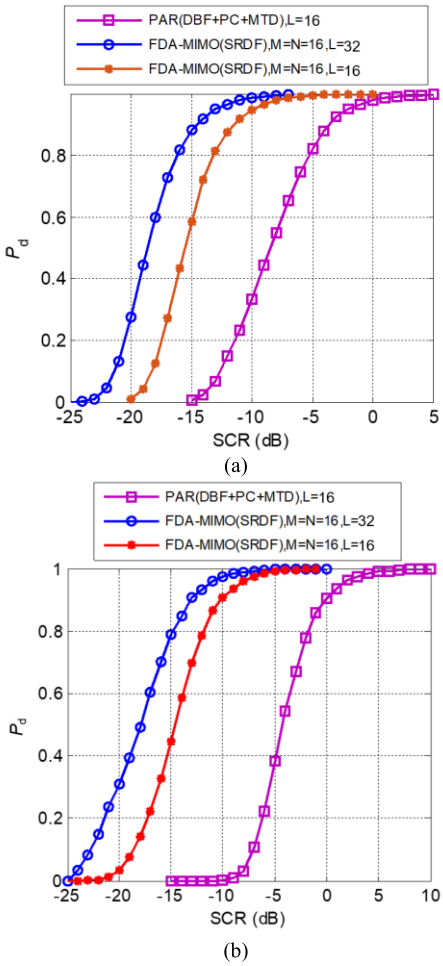

FIGURE 21. Detection probability of PAR and FDA-MIMO radar in clutter background ($P_{fa} = 10^{-3}$). (a) Uniformly moving target. (b) Accelerated moving target.

different dimensions) are used and accumulated, the SRDF-based detection method shows obvious advantage over the traditional methods using PAR (digital beamforming (DBF), pulse compression (PC), MTD). Under the same detection probability $P_d = 0.8$, the SCR threshold for the FDA-MIMO with $L = 16$ is about −15 dB, which is smaller for 10 dB than the corresponding thresholds of PAR. In addition, compared with the P_d curves of SRDF with different sample number, we can see that more samples can help improve the detection performance. Compared with the detection curves of uniformly moving target and accelerated moving target, it can be found that due to the Doppler migration, the detection probability has about 0.2 loss for FDA-MIMO and 0.4 loss for PAR. This is because that the MTD of PAR is based on the filter banks processing via FFT.

3) PERFORMANCES FOR MOTION PARAMETERS ESTIMATION

Under the same condition of Fig. 17, the estimation results and the computation time of PAR and FDA-MIMO using the proposed SRDF are shown in Tab. 1. The estimation

TABLE 1. The comparisons of motion parameters estimation. (The same parameter of accelerated moving target in Fig. 17, SCR = −15dB).

	$\hat{f}_0$(Hz)	Δf_0(Hz)	$\hat{\mu}$(Hz/s)	$\Delta\mu$(Hz/s)	$\overline{t}(s)$
PAR[1]	-272	12	——	——	4.89
PAR[2]	-265	5	10.6	2.8	10.53
FDA-MIMO	**-260**	**0**	**13.3**	**0.1**	**12.64**

*Main configuration of the computer: Intel Core i7-4790 3.6GHz CPU; 16G RAM; Matlab R2014a.
PAR[1]: DBF+PC+MTD;
PAR[2]: DBF+PC+FRFT;
FDA-MIMO: SRDF (SFRFT)

performance is compared by computing the absolute error, which is defined as

$$|\Delta f_0| = \left|f_0 - \hat{f}_0\right|, \quad |\Delta\mu| = \left|\mu - \hat{\mu}\right| \tag{32}$$

Tab. 1 demonstrates that the FDA-MIMO outperforms the traditional PAR greatly in low SCR environment due to the good concentration and high-resolution ability of SRDF. However, the proposed method costs more time due to the joint optimization process in 3D domains. Hence, a more efficient method of SRDF is needed in the future work.

V. CONCLUSIONS

FDA radar has received much attention in recent years due to its range-dependent transmit beampattern, but it has several problems for signal processing, such as angle and range coupling and Doppler processing for moving target. In this paper, FDA-MIMO radar is employed for low-observable moving target detection, and a novel three-dimensional processing method, i.e., SRDF, is proposed for coherent integration and high-resolution estimation. The concept and signal model of SRDF for FDA-MIMO is established. Then, we provide the implementation of SRDF and use STFD to achieve high-resolution representation of Doppler, which is a possible solution for real applications. Finally, simulations under noise and clutter environment show that the proposed method can achieve 3D parameters estimation and has better ability for integration and clutter suppression. It has the advantages of high integration gain, high-resolution, anti-clutter, etc.. More investigations on real experiments for different motions will be carried out in future work.

ACKNOWLEDGMENT

The authors would like to thank the anonymous reviewers for the valuable comments and suggestions.

REFERENCES

[1] G. Zhao, Q. Liang, and T. S. Durrani, "UWB radar target detection based on hidden Markov models," *IEEE Access*, vol. 6, pp. 28702–28711, 2018.
[2] X. Wang, E. Aboutanios, and M. G. Amin, "Slow radar target detection in heterogeneous clutter using thinned space-time adaptive processing," *IET Radar, Sonar Navigat.*, vol. 10, no. 4, pp. 726–734, 2016.
[3] X. Chen, Y. Huang, N. Liu, J. Guan, and Y. He, "Radon-fractional ambiguity function-based detection method of low-observable maneuvering target," *IEEE Trans. Aerosp. Electron. Syst.*, vol. 51, no. 2, pp. 815–833, Apr. 2015.
[4] X. Chen, J. Guan, N. Liu, W. Zhou, and Y. He, "Detection of a low observable sea-surface target with micromotion via the radon-linear canonical transform," *IEEE Geosci. Remote Sens. Lett.*, vol. 11, no. 7, pp. 1225–1229, Jul. 2014.
[5] J. Carretero-Moya, J. Gismero-Menoyo, A. Asensio-López, and A. Blanco-Del-Campo, "Small-target detection in high-resolution heterogeneous sea-clutter: An empirical analysis," *IEEE Trans. Aerosp. Electron. Syst.*, vol. 47, no. 3, pp. 1880–1898, Jul. 2011.
[6] X. Li, G. Cui, W. Yi, and L. Kong, "Fast coherent integration for maneuvering target with high-order range migration via TRT-SKT-LVD," *IEEE Trans. Aerosp. Electron. Syst.*, vol. 52, no. 6, pp. 2803–2814, Dec. 2016.
[7] G. Cui, L. Kong, X. Yang, and J. Yang, "Distributed target detection with polarimetric MIMO radar in compound-Gaussian clutter," *Digit. Signal Process.*, vol. 22, no. 3, pp. 430–438, 2012.
[8] P. Huang, G. Liao, Z. Yang, X.-G. Xia, J.-T. Ma, and J. Ma, "Long-time coherent integration for weak maneuvering target detection and high-order motion parameter estimation based on keystone transform," *IEEE Trans. Signal Process.*, vol. 64, no. 15, pp. 4013–4026, Aug. 2016.
[9] P.-L. Shui, M. Liu, and S.-W. Xu, "Shape-parameter-dependent coherent radar target detection in K-distributed clutter," *IEEE Trans. Aerosp. Electron. Syst.*, vol. 52, no. 1, pp. 451–465, Feb. 2016.
[10] F. Millioz and M. Davies, "Sparse detection in the chirplet transform: Application to FMCW radar signals," *IEEE Trans. Signal Process.*, vol. 60, no. 6, pp. 2800–2813, Jun. 2012.
[11] Y. Li, L. Wu, and N. Zhang, "A CFAR detector based on a robust combined method with spatial information and sparsity regularization in non-homogeneous Weibull clutter," *IEEE Access*, vol. 6, pp. 16279–16293, 2018.
[12] X. Chen, Y. Huang, J. Guan, and Y. He, "Radar micro-Doppler signal detection and extraction via short-time sparse fractional Fourier transform," in *Proc. Int. Conf. Radar Syst. (Radar)*, 2017, pp. 1–4.
[13] W. L. Melvin, "Space-time adaptive radar performance in heterogeneous clutter," *IEEE Trans. Aerosp. Electron. Syst.*, vol. 36, no. 2, pp. 621–633, Apr. 2000.
[14] X. Chen, J. Guan, Y. He, and J. Zhang, "Detection of low observable moving target in sea clutter via fractal characteristics in fractional Fourier transform domain," *IET Radar, Sonar Navigat.*, vol. 7, no. 6, pp. 635–651, Jul. 2013.
[15] V. C. Chen, F. Li, S.-S. Ho, and H. Wechsler, "Micro-Doppler effect in radar: Phenomenon, model, and simulation study," *IEEE Trans. Aerosp. Electron. Syst.*, vol. 42, no. 1, pp. 2–21, Jan. 2006.
[16] M. Liu, L. Chenlei, and Z. Shuqing, "Joint space-time-frequency method based on fractional Fourier transform to estimate moving target parameters for multistatic synthetic aperture radar," *IET Signal Process.*, vol. 7, no. 1, pp. 71–80, Feb. 2013.
[17] S. Ahmed and M.-S. Alouini, "MIMO-radar waveform covariance matrix for high SINR and low side-lobe levels," *IEEE Trans. Signal Process.*, vol. 62, no. 8, pp. 2056–2065, Apr. 2014.
[18] M. Davis, G. Showman, and A. Lanterman, "Coherent MIMO radar: The phased array and orthogonal waveforms," *IEEE Aerosp. Electron. Syst. Mag.*, vol. 29, no. 8, pp. 76–91, Aug. 2014.
[19] X. Chen, J. Guan, N. Liu, and Y. He, "Maneuvering target detection via radon-fractional Fourier transform-based long-time coherent integration," *IEEE Trans. Signal Process.*, vol. 62, no. 4, pp. 939–953, Feb. 2014.
[20] W.-K. Gu, D.-W. Wang, and X.-Y. Ma, "High speed moving target detection using distributed OFDM-MIMO phased radar," in *Proc. 12th Int. Conf. Signal Process. (ICSP)*, Oct. 2014, pp. 2087–2091.
[21] L. Wan, X. Kong, and F. Xia, "Joint range-Doppler-angle estimation for intelligent tracking of moving aerial targets," *IEEE Internet Things J.*, vol. 5, no. 3, pp. 1625–1636, Jun. 2018.
[22] C. Wen, J. Peng, Y. Zhou, and J. Wu, "Enhanced three-dimensional joint domain localized STAP for airborne FDA-MIMO radar under dense false-target jamming scenario," *IEEE Sensors J.*, vol. 18, no. 10, pp. 4154–4166, May 2018.
[23] W.-Q. Wang, H. C. So, and A. Farina, "An overview on time/frequency modulated array processing," *IEEE J. Sel. Topics Signal Process.*, vol. 11, no. 2, pp. 228–246, Mar. 2017.
[24] T. Higgins and S. D. Blunt, "Analysis of range-angle coupled beamforming with frequency-diverse chirps," in *Proc. Int. Waveform Diversity Design Conf.*, Feb. 2009, pp. 140–144.

[25] C. Wang, J. Xu, G. Liao, X. Xu, and Y. Zhang, "A range ambiguity resolution approach for high-resolution and wide-swath SAR imaging using frequency diverse array," *IEEE J. Sel. Topics Signal Process.*, vol. 11, no. 2, pp. 336–346, Mar. 2017.

[26] W.-Q. Wang, "Frequency diverse array antenna: New opportunities," *IEEE Antennas Propag. Mag.*, vol. 57, no. 2, pp. 145–152, Apr. 2015.

[27] P. Baizert, T. B. Hale, M. A. Temple, and M. C. Wicks, "Forward-looking radar GMTI benefits using a linear frequency diverse array," *Electron. Lett.*, vol. 42, no. 22, pp. 1311–1312, 2006.

[28] J. Xu, S. Zhu, and G. Liao, "Range ambiguous clutter suppression for airborne FDA-STAP radar," *IEEE J. Sel. Topics Signal Process.*, vol. 9, no. 8, pp. 1620–1631, Dec. 2015.

[29] B. Chen, X. Chen, Y. Huang, and J. Guan, "Transmit beampattern synthesis for the FDA radar," *IEEE Antennas Wireless Propag. Lett.*, vol. 17, no. 1, pp. 98–101, Jan. 2018.

[30] P. Antonik, M. C. Wicks, H. D. Griffiths, and C. J. Baker, "Range-dependent beamforming using element level waveform diversity," in *Proc. Int. Waveform Diversity Design Conf.*, Jan. 2006, pp. 1–6.

[31] M. Secmen, S. Demir, A. Hizal, and T. Eker, "Frequency diverse array antenna with periodic time modulated pattern in range and angle," in *Proc. IEEE Radar Conf.*, Apr. 2007, pp. 427–430.

[32] P. F. Sammartino, C. J. Baker, and H. D. Griffiths, "Frequency diverse MIMO techniques for radar," *IEEE Trans. Aerosp. Electron. Syst.*, vol. 49, no. 1, pp. 201–222, Jan. 2013.

[33] A. M. Jones and B. D. Rigling, "Frequency diverse array radar receiver architectures," in *Proc. Int. Waveform Diversity Design Conf. (WDD)*, Jan. 2012, pp. 211–217.

[34] A. Basit, I. M. Qureshi, W. Khan, and S. U. Khan, "Cognitive frequency offset calculation for frequency diverse array radar," in *Proc. 12th Int. Bhurban Conf. Appl. Sci. Technol. (IBCAST)*, Jan. 2015, pp. 641–645.

[35] W. Khan, I. M. Qureshi, A. Basit, and W. Khan, "Range-bins-based MIMO frequency diverse array radar with logarithmic frequency offset," *IEEE Antennas Wireless Propag. Lett.*, vol. 15, pp. 885–888, 2016.

[36] Y. Liu, H. Ruan, L. Wang, and A. Nehorai, "The random frequency diverse array: A new antenna structure for uncoupled direction-range indication in active sensing," *IEEE J. Sel. Topics Signal Process.*, vol. 11, no. 2, pp. 295–308, Mar. 2017.

[37] J. Xu, G. Liao, Y. Zhang, H. Ji, and L. Huang, "An adaptive range-angle-Doppler processing approach for FDA-MIMO radar using three-dimensional localization," *IEEE J. Sel. Topics Signal Process.*, vol. 11, no. 2, pp. 309–320, Mar. 2017.

[38] S. Qin, Y. D. Zhang, M. G. Amin, and F. Gini, "Frequency diverse coprime arrays with coprime frequency offsets for multitarget localization," *IEEE J. Sel. Topics Signal Process.*, vol. 11, no. 2, pp. 321–335, Mar. 2017.

[39] C. Cui, J. Xu, R. Gui, W.-Q. Wang, and W. Wu, "Search-free DOD, DOA and range estimation for bistatic FDA-MIMO radar," *IEEE Access*, vol. 6, pp. 15431–15445, 2018.

[40] J. Xiong, W.-Q. Wang, and K. Gao, "FDA-MIMO radar range–angle estimation: CRLB, MSE, and resolution analysis," *IEEE Trans. Aerosp. Electron. Syst.*, vol. 54, no. 1, pp. 284–294, Feb. 2018.

[41] W.-Q. Wang, "Moving-target tracking by cognitive RF stealth radar using frequency diverse array antenna," *IEEE Trans. Geosci. Remote Sens.*, vol. 54, no. 7, pp. 3764–3773, Jul. 2016.

[42] B. Jokanovic and M. Amin, "Reduced interference sparse time-frequency distributions for compressed observations," *IEEE Trans. Signal Process.*, vol. 63, no. 24, pp. 6698–6709, Dec. 2015.

[43] X. Chen, J. Guan, and Y. He, "High resolution extraction of radar micro-Doppler signature using sparse time-frequency distribution," in *Proc. 32nd Gen. Assem. Sci. Symp. Int. Union Radio Sci. (URSI GASS)*, Aug. 2017, pp. 1–4.

[44] K. V. Rangarao and S. Venkatanarasimhan, "Gold-MUSIC: A variation on music to accurately determine peaks of the spectrum," *IEEE Trans. Antennas Propag.*, vol. 61, no. 4, pp. 2263–2268, Apr. 2013.

[45] J. Xie, Z. Wang, Z. Ji, and T. Quan, "High-resolution ocean clutter spectrum estimation for shipborne HFSWR using sparse-representation-based MUSIC," *IEEE J. Ocean. Eng.*, vol. 40, no. 3, pp. 546–557, Jul. 2015.

[46] P. R. Gill, A. Wang, and A. Molnar, "The in-crowd algorithm for fast basis pursuit denoising," *IEEE Trans. Signal Process.*, vol. 59, no. 10, pp. 4595–4605, Oct. 2011.

[47] S. Liu *et al.*, "Sparse discrete fractional Fourier transform and its applications," *IEEE Trans. Signal Process.*, vol. 62, no. 24, pp. 6582–6595, Dec. 2014.

[48] A. C. Gilbert, P. Indyk, M. Iwen, and L. Schmidt, "Recent developments in the sparse Fourier transform: A compressed Fourier transform for big data," *IEEE Signal Process. Mag.*, vol. 31, no. 5, pp. 91–100, Sep. 2014.

XIAOLONG CHEN (M'12) was born in Yantai, Shandong, China, in 1985. He received the bachelor's and master's degrees in signal and information processing and the Ph.D. degree in radar signal processing from Naval Aviation University (NAU) in 2010 and 2014, respectively. From 2015 to 2017, he was a Lecturer with the Marine Target Detection Research Group, NAU, where he lectures radar principle. He is currently an Associate' Professor with NAU.

He has published over 60 academic articles, two book chapters, and holds 18 national invention patents. His current research interests include marine target detection, micro-Doppler, and sea clutter suppression. He has given over 20 speeches of radar signal processing especially marine target.

Dr. Chen has been a member of the 2015 and 2018 IET International Radar Conference Technical Committees. In 2016, he was selected in the Young Talents Program of the China Association for Science and Technology, and received the Excellent Doctor Dissertation of CIE. In 2017, he received the Chinese Patent Award. He received three excellent papers in the 2016 International Radar Conference, the 2017 EAI International Conference on Machine Learning and Intelligent Communications (MLICOM), and the 14th National Radar Conference, respectively. He was the Section Chair of the 2016 International Conference on Mathematical Characterization, Analysis and Applications of Complex Information, 2017 MLICOM, and the 2017 International Conference on Radar Systems, U.K. He is an Associate Editor of the journal IEEE Access and frequently a Reviewer of IEEE SPL, IEEE TGRS, IEEE GRSL, IEEE JSTARS, IET RSN, IET SP, IET EL, and DSP, and many international conferences.

BAOXIN CHEN was born in Shandong, China, in 1990. He received the M.S. degree in automation from Logistical Engineering University in 2013. He is currently pursuing the Ph.D. degree with the NAU of Information and Communication Engineering, Yantai, China. His main research interests include MIMO/FDA radar signal processing, adaptive array signal processing, and beamforming.

JIAN GUAN (M'07) received the Ph.D. degree in electronic engineering from Tsinghua University, Beijing, China in 2000. He is currently a Professor of NAU.

He has authored numerous papers in his areas of expertise and holds 21 national invention patents. He is the authors of two books related to radar detection. His research interests include radar target detection and tracking, image processing, and information fusion. Dr. Guan is a Senior Member of CIE and a Committee Member of the Radio Positioning Technology Branch, CIE. He received the prize of the National Excellent Doctoral Dissertation and the Realistic Outstanding Youth Practical Engineering Award of CAST, and he was selected for the National Talents Engineering of the Ministry of Personnel of China. He has served in the technical committee of many international conferences on radar. He is on the Editorial Board of many radar related journals.

YONG HUANG was born in Shandong, China, in 1978. He received the M.S. and Ph.D. degrees in information and communication engineering from NAU, in 2005 and 2010, respectively. From 2011 to 2016, he was a Lecturer with the Department of Electronic and Information Engineering, NAU, where he is currently an Associate Professor.

His current research interests include radar signal processing and clutter modeling.

YOU HE was born in Jilin, China, in 1956. He received the Ph.D. degree in electronic engineering from Tsinghua University, Beijing, China, in 1997. He is currently a Professor with NAU. He has published over 300 academic articles. He is the author of *Radar Target Detection and CFAR Processing* (Tsinghua University Press), *Multisensor Information Fusion with Applications*, and *Radar Data Processing With Applications* (Publishing House of Electronics Industry). His current research interests include detection and estimation theory, CFAR processing, distributed detection theory, and multisensor information fusion.

Dr. He has been a Fellow Member of the Chinese Institute of Electronic since 2013. In 2017, he received the top prize in science and technology of Shandong Province. He currently serves on the Editorial Board of the *Journal of Data Acquisition & Processing*, *Modern Radar*, *Fire Control & Command Control*, and *Radar Science and Technology*.